Diffusion weighted imaging and diffusion tensor imaging in the evaluation of transplanted kidneys

Stefano Palmucci [a],*, Giuseppina Cappello [a], Giancarlo Attinà [a], Pietro Valerio Foti [a],
Rita Olivia Anna Siverino [a], Federica Roccasalva [a], Marina Piccoli [a], Nunziata Sinagra [b],
Pietro Milone [a], Massimiliano Veroux [b], Giovanni Carlo Ettorre [a]

[a] *Radiodiagnostic and Radiotherapy Unit, University Hospital "Policlinico-Vittorio Emanuele", Via Santa Sofia 78, 95123 Catania, Italy*
[b] *Vascular Surgery and Organ Transplant Unit, Department of Surgery, Transplantation and Advanced Technologies, University Hospital "Policlinico-Vittorio Emanuele", Via Santa Sofia 78, 95123 Catania, Italy*

Abstract

Objective: The aim of this study is to investigate the relation between renal indexes and functional MRI in a population of kidney transplant recipients who underwent MR with diffusion-weighted imaging (DWI) and diffusion tensor imaging (DTI) of the transplanted graft.

Method: Study population included 40 patients with single kidney transplant. The patients were divided into 3 groups, on the basis of creatinine clearance (CrCl) values calculated using Cockcroft-Gault formula: group A, including patients with normal renal function (CrCl ≥ 60 mL/min); group B, which refers to patients with moderate renal impairment (CrCl > 30 but <60 mL/min); and, finally, group C, which means severe renal deterioration (CrCl ≤ 30 mL/min). All patients were investigated with a 1.5 Tesla MRI scanner, acquiring DWI and DTI sequences. A Mann–Whitney U test was adopted to compare apparent diffusion coefficients (ADCs) and fractional anisotropy (FA) measurements between groups. Receiver operating characteristic (ROC) curves were created for prediction of normal renal function (group A) and renal failure (group C). Pearson correlation was performed between renal clearance and functional imaging parameter (ADC and FA), obtained for cortical and medullar regions.

Results: Mann–Whitney U test revealed a highly significant difference ($p < 0.01$) between patients with low CrCl (group C) and normal CrCl (group A) considering both medullar ADC and FA and cortical ADC. Regarding contiguous groups, the difference between group B and C was highly significant ($p < 0.01$) for medullar ADC and significant ($p < 0.05$) for cortical ADC and medullar FA. No difference between these groups was found considering cortical FA. Analyzing groups A and B, we found a significant difference ($p < 0.05$) for medullar both ADC and FA, while no difference was found for cortical ADC and FA.

Strongest Pearson correlation was found between CrCl and medullar ADC ($r = 0.65$). For predicting normal renal function or severe renal impairment, highest values of AUC were observed using medullar ADC cut-off values (respectively 0.885 and 0.871); medullar FA showed also high accuracy (respectively 0.831 and 0.853).

Conclusions: DWI and DTI are promising tools for non-invasive monitoring of renal function; medullar ADC proved to be the best parameter for renal function assessment.

1. Introduction

Renal graft function is monitored using clinical parameters – such as serum creatinine, creatinine clearance – and imaging modalities, mainly represented by ultrasound, ecocolor-doppler and scintigraphy; however, the assessment of renal disease requires parenchymal biopsy to make a correct diagnosis, grading also the level of damage. Renal biopsy is an invasive

---

procedure, not free from complications (hemorrhage, infection, etc.). In a recent study by Franke et al., a not-irrelevant number of complications (perirenal/retroperitoneal bleeding, hematuria, arterio-venous fistula) have been found; indeed, the complication rate was 4.1% [1].

The possibility of investigating renal function is one of the most recent goals of functional MRI; namely, this potentiality has been gradually increased in importance due to the fact that gadolinium enhanced MRI has a non-negligible degree of nephrotoxicity [2,3].

In the past decade, several articles have pointed out the role of functional MRI in the evaluation of kidney diseases [4]. DWI has been used to characterize focal renal lesions [5], and to investigate renal function, either in normal kidneys [6] or renal graft also [7].

All renal functions, such as glomerular filtration, tubular reabsorption and secretion, are based on water transportation [8]. Thus, quantification of Brownian motions measured by DWI may provide a functional assessment of renal parenchyma. Diffusion and perfusion effects are expressed by a numerical value, named ADC, which decreases with restriction of diffusion of water molecules. ADC is defined as "an average index of how freely water can move within a voxel (i.e. averaged across all tissue structures and compartments within the voxel) and hence the term apparent" [9].

However, molecular motility may not be the same in all directions, leading to a certain anisotropy. It can be due for example to an obstacle limiting molecular movements or to the anatomic orientation of the structures of the tissue. DTI is able to evaluate diffusion anisotropy measuring diffusion of water molecules for each single direction of the gradient pulses. DTI allows us to obtain in vivo information about oriented tissues, such as brain white matter, muscles and myocardium [10]. Its role has been emphasized in brain study, particularly in patients with brain tumors to evaluate displacement or interruption of white matter pathways, and in demyelinating disease to detect subtle changes in myelin fibers integrity [11]. As in brain white matter, also in renal medulla there is an intrinsic orientation of the structures because it is assembled in tubuli and ducti with parallel coarse. Thus, several studies have pointed out that normal renal architecture suggest a different evaluation of diffusion direction using DTI, that could be able to evaluate the degree of medullary anisotropy [12].

The purpose of our study was to evaluate the usefulness of DWI and DTI in assessing allograft dysfunction correlating ADC and FA values with laboratory data; diagnostic accuracy of ADC and FA is calculated, in order to investigate which is the most useful parameter for the evaluation of renal function.

2. Material and methods

2.1. Study population

Patients were enrolled between September 2014 and January 2015. This study was approved by our internal ethics committee and a written informed consent was obtained from all patients before MRI.

Study population included forty patients with single kidney transplant (24 males, 16 females) with a mean age of 50.6 years (range, 17–78). 32 of them received transplant from deceased donor, 8 from living donor. A serum creatinine value was collected no more than 36 h before or after MRI examination.

Patients received a standard immunosuppressive protocol with a calcineurin inhibitor (tacrolimus in 27 and cyclosporine in 13), mycophenolatemofetil and steroids. None of the patients experienced an episode of acute rejection during the study period. MRI examinations were performed at a mean post-transplant time of 3.8 years (range, 8 days-22.8 years). No patients were excluded from this study.

Kidney transplantations, clinical management and follow-up were performed by the same surgical team. All transplanted kidneys were placed in the right iliac fossa with vascular anastomoses to the common or external iliac vessels. The patients were divided into 3 groups, on the basis of CrCl values calculated using Cockcroft-Gault formula:

- group A, patients with CrCl ≥ 60 mL/min;
- group B, patients with CrCl > 30 but <60 mL/min;
- group C, patients with CrCl ≤ 30 mL/min.

2.2. MRI protocol

All examinations were performed using a 1.5 Tesla scanner (SignaHDxt, General Electric). Images were acquired with an 8-channels array coil (8 channel body coil), using the lower configuration; sequences were not respiratory-triggered, so that no "respiratory" belt was used.

Unenhanced T1 and T2-weighted sequences were performed before DTI in order to obtain a morphological evaluation of transplanted kidneys. Axial sequences were positioned perpendicularly to the major axis of the kidney (Fig. 1). No intravenous hypotonic agent was administrated. Protocol examination included:

- Axial T2-weighted Fast Recovery Fast Spin Echo sequence, obtained with a TR = 3200 ms, TE = 110 ms, thickness = 5 mm, gap interval = 0.5 mm, Number of Excitations = 4, matrix = 320 × 224, Field of View = 36–40;
- Coronal T2-weighted Fast Recovery Fast Spin Echo sequence, obtained with a TR = 3100 ms, TE = 103 ms, thickness = 3 mm, gap interval = 0.3 mm, Number of Excitations = 4, matrix = 320 × 224;
- Diffusion-weighted sequences, obtained by Single Shot Echo Planar Imaging technique, using a b value of 500. Namely, acquisition parameters were the following: TR = 3000 ms; TE = 40–79 ms; Number of Excitations = 2; acceleration factor = 2; EPI factor = 80; thickness = 5 mm; spacing = 1 mm; Field of View = 34–42; matrix = 128 × 128, acquisition time = 1 min 42 s.
- DTI was acquired using a "free-breathing" Single Shot Echo Planar Imaging technique, with diffusion gradient active for 6 directions. Acquisition parameters were: TR = 7500 ms;
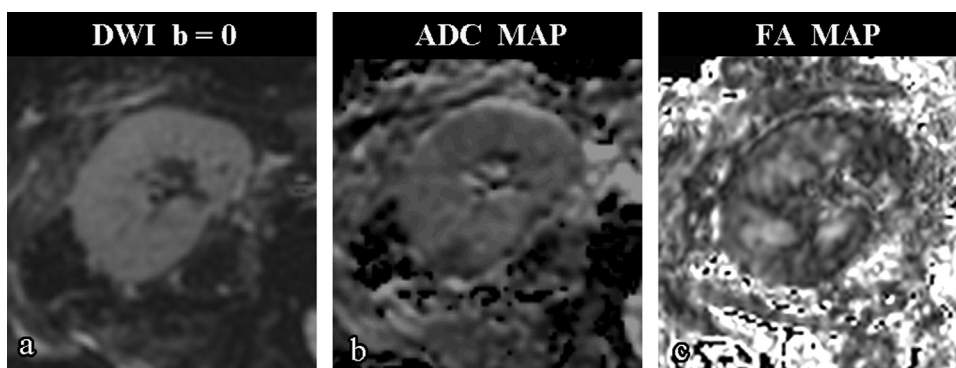
Fig. 1. Axial b = 0 (a), ADC map (b) and FA map (c) images of a 52-year old woman with good renal function (CrCl = 104 mL/min). FA map shows good visual differentiation between cortical and medullar parenchyma.

TE = 86 ms; Number of Excitations = 4; acceleration factor = 2; EPI factor = 80; thickness = 6 mm; spacing = 1 mm; Field of View = 34–42 cm; matrix = 128 × 128, acquisition time = 3 min 38 s.

2.3. Image analysis

Morphological evaluation of the transplanted kidney was performed using axial and coronal T2-weighted sequences. We investigated both vascular and non vascular complications that may affect transplanted kidneys, such as focal or diffuse parenchymal signal alterations, perirenal fluid collections, lymphoceles, arterial, venous and collecting system abnormalities. These conditions, which can occur both in the early postoperative period and in the long-term, must be recognized because they influence the transplanted patients' outcome. ADC and FA were calculated by placing a circular ROI both in the cortical and in the medulla for each transplanted kidney in three different levels: upper, middle and lower third. For positioning of cortical and medullar ROIs, anatomical T2-weighted acquisitions and b = 0 images were used.

The ROIs were always placed avoiding all possible inclusions of vessels and focal lesions. A mean score was obtained for both cortical and medullar ADC values and for both cortical and medullar FA values. Post-processing was performed using the General Electric Functool software package (GE Healthcare®).

2.4. Statistical analysis

Statistical analysis was performed using Win-Stat Software and a MedCalc program (MedCalc version 11.4.4.0, MedCalc Software bvba, Mariakerke, Belgium).

Cortical and medullar ADC and FA mean values were compared among the three different groups using the Mann–Whitney U test; $p < 0.05$ was considered statistically significant. Both cortical and medullar ADC and FA were correlated to Cr Cl using Pearson linear regression.

Lastly, optimal ADC and FA threshold values for group membership were determined by ROC analysis, calculating corresponding sensitivities, specificities and diagnostic accuracies.

3. Results

3.1. Qualitative analysis

Morphologic imaging showed absence of renal disease in 23 patients. No vascular complications – such as renal artery stenosis or partial vein thrombosis – were found. MRI demonstrated 5 fluid collections and 6 lymphoceles located in renal graft area, behind the iliac vessels or near the inguinal region. A renal mass was found in 1 patient. In 2 patients renal pelvis dilatation was demonstrated. 3 cases of pyelonephritis were also found.

3.2. Quantitative analysis

The patients' distribution into 3 groups, on the basis of CrCl, was as follow (Table 1): 10 patients in group A (4 males and 6 females, with a mean age of 51.2 years); 12 patients in group B (8 males and 4 females, with a mean age of 48.7 years); 18 patients in group C (12 males and 6 females, with a mean age of 51.6 years).

Comparing mean values of cortical ADC (Fig. 2), we did not observe a significant difference ($p = 0.06$) between groups A and B, whereas we found a highly significant difference ($p < 0.01$) in the comparison between groups A and C, and a statistically significant difference between groups B and C ($p = 0.02$).

Comparing mean values of medullar ADC (Fig. 3) we observed a significant difference ($p = 0.02$) between groups A and B; a highly significant difference ($p < 0.01$) was reported between groups A and C, and between groups B and C.

Comparing mean values of cortical FA (Fig. 4) we did not observe a significant difference comparing groups A and B ($p = 0.74$), groups A and C ($p = 0.63$), and groups B and C ($p = 0.98$).

Comparing mean values of medullar FA (Fig. 5) between groups A and B, we observed a significant difference ($p = 0.03$). In the comparison between groups A and C, we observed a highly significant difference ($p < 0.01$). For medullar FA, the difference reported between groups B and C, was also significant ($p = 0.02$).

Pearson correlation test showed a strong positive correlation between CrCl and medullar FA (Fig. 6a), with a coefficient of 0.62 while cortical FA showed no correlation with r value < 0.1. For ADC values a positive correlation was found between

Table 1
Study population: CrCl, cortical ADC, medullar ADC, Cortical FA and medullar FA mean values of each patient.

Group A CrCl ≥60 mL/min						Group B CrCl >30 < 60 mL/min						Group C CrCl ≤30 mL/min					
PT	ClCr	ADC cort	ADC med	FA cort	FA med	PT	ClCr	ADC cort	ADC med	FA cort	FA med	PT	ClCr	ADC cort	ADC med	FA cort	FA med
2	67	2.31	2.36	0.265	0.233	3	45	1.75	2.17	0.278	0.230	1	17	2.63	2.30	0.213	0.149
4	94	2.57	2.41	0.288	0.347	6	55	2.36	2.09	0.203	0.154	5	21	2.19	2.40	0.264	0.139
7	71	2.39	2.54	0.315	0.231	10	42	2.14	2.36	0.179	0.202	9	4	2.23	1.82	0.203	0.156
8	104	2.56	2.18	0.187	0.311	11	36	2.63	1.93	0.232	0.263	12	15	1.62	1.75	0.245	0.172
13	72	2.19	2.48	0.217	0.340	17	34	2.13	1.90	0.229	0.204	14	7	1.97	1.83	0.319	0.177
15	116	2.90	2.55	0.193	0.267	20	50	2.10	2.16	0.074	0.261	16	28	1.62	1.79	0.280	0.100
19	92	2.48	2.55	0.204	0.262	22	32	1.99	2.03	0.171	0.142	18	30	2.16	2.36	0.224	0.284
27	99	2.26	2.40	0.267	0.197	25	44	2.04	2.61	0.289	0.190	21	26	1.83	1.95	0.176	0.225
31	74	2.20	2.46	0.183	0.474	29	34	2.13	2.30	0.223	0.222	23	18	1.88	2.08	0.238	0.213
34	93	1.89	1.96	0.188	0.213	33	51	2.54	2.39	0.318	0.260	24	10	2.14	1.66	0.201	0.103
						36	57	2.36	2.23	0.246	0.328	26	20	1.86	1.92	0.152	0.156
						39	52	1.88	2.04	0.151	0.225	28	9	1.96	1.91	0.166	0.118
												30	15	1.87	1.79	0.120	0.111
												32	11	1.91	1.71	0.193	0.103
												35	30	1.80	1.98	0.294	0.191
												37	24	1.75	1.94	0.178	0.197
												38	29	1.70	1.84	0.202	0.275
												40	19	1.50	1.64	0.305	0.190

Abbreviations: PT = patient; CrCl = creatinine clearance; ADC cort = mean cortical ADC; ADC med = mean medullar ADC; FA cort = mean cortical FA; FA med = mean medullar FA.
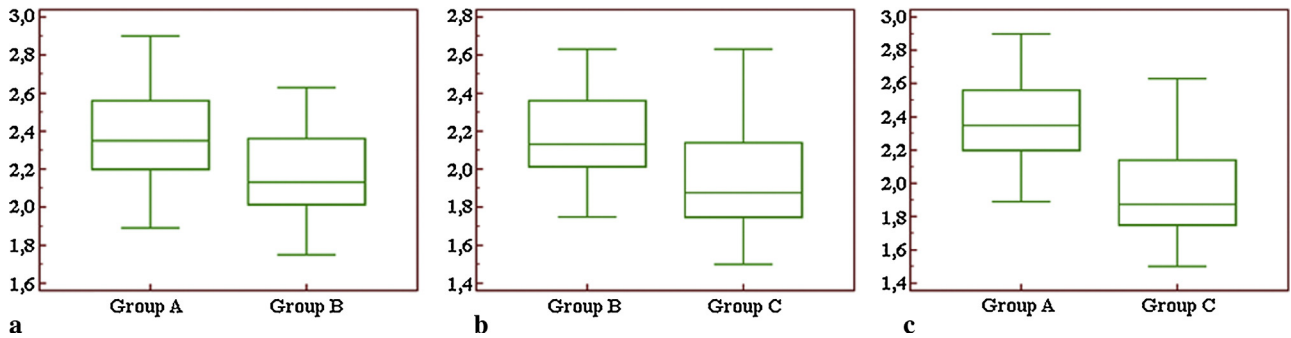
Cortical ADC

Fig. 2. Box-and-whisker plot for cortical ADC values (a–c): considering cortical ADC measurement, we found a significant statistical difference only comparing groups B and C (b) and groups A and C (c). No difference was observed for cortical ADC measurements between group A and B (a).
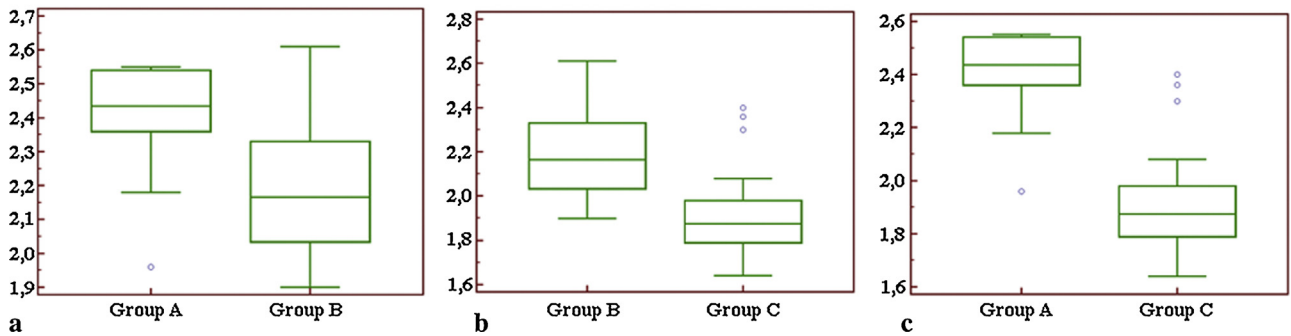
Medullar ADC

Fig. 3. Box-and-whisker plot for medullar ADC measurements (a–c): comparing mean values between groups A and B (a) we observed a significant difference ($p = 0.02$). Comparing groups B and C (b), the difference was highly significant, with a $p < 0.01$. Highly significant difference ($p < 0.01$) was reported in the comparison between groups A and C (c).

medullar ADC and CrCl, with *r* coefficient of 0.66 (Fig. 6b). A moderate positive correlation was reported between cortical ADC and CrCl, with *r* coefficient of 0.57.

ROC analysis for prediction of normal clearance values or advanced renal impairment using ADC and FA mean values, are shown in Figs. 7 and 8 respectively.

In the prediction of renal low clearance values (patients of group C), using a threshold cortical ADC value $\leq 1.97 \times 10^{-3}$ mm²/s, the ROC curve showed an AUC of 0.814, a 95% Confidence Interval (CI) for the area = 0.660–0.919, with sensitivity of 72.2% and specificity of 86.4%; for prediction of normal renal function (group A), using a threshold
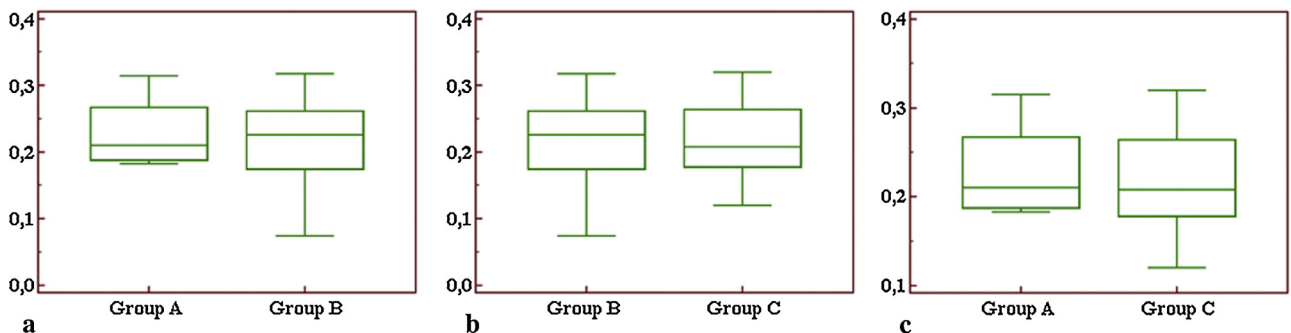
Cortical FA

Fig. 4. Box-and-whisker plot for cortical FA values (a–c): no difference was observed comparing mean values between groups A and B (a), between groups B and C (b) and between groups A and C (c).
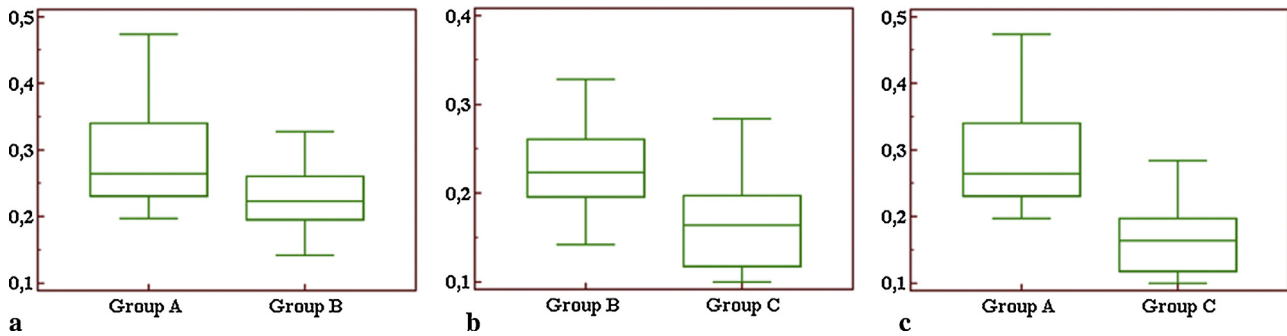
Medullar FA

Fig. 5. Box-and-whisker plot for medullar FA measurements (a–c): comparing mean values between groups A and B (a), we observed a significant difference ($p = 0.03$). In comparing groups B and C (b), the difference was also significant ($p = 0.02$). In the comparison between groups A and C (c), we observed a highly significant difference ($p < 0.01$).

cortical ADC value $>2.16 \times 10^{-3}$ mm^2/s, the ROC curve showed an AUC of 0.832, 95% CI = 0.680–0.931, with sensitivity of 90% and specificity of 76.7%.

In the prediction of renal low clearance values (group C), using a threshold medullar ADC value $\leq 1.98 \times 10^{-3}$ mm^2/s, 95% CI = 0.727–0.956, the ROC curve showed an AUC of 0.871, with sensitivity of 77.8% and specificity of 86.4%. For the prediction of renal normal clearance values (patients of group A) using a threshold medullar ADC value $>2.3 \times 10^{-3}$ mm^2/s, 95% CI = 0.744–0.964, the ROC curve showed an AUC of 0.885, with sensitivity of 80% and specificity of 83.3%.

In the prediction of renal low clearance values (patients of group C) using a threshold cortical FA value $\leq 0.178 \times 10^{-3}$ mm^2/s, 95% CI = 0.363–0.686, the ROC curve showed an AUC of 0.527, with sensitivity of 27.8% and specificity of 86.4%. For prediction of renal normal clearance values (patients of group A) using a threshold cortical FA value $>0.179 \times 10^{-3}$ mm^2/s, 95% CI = 0.385–0.707, the ROC curve showed an AUC of 0.550, with sensitivity of 100% and specificity of 30%.

In the prediction of renal low clearance values (patients of group C) using a threshold medullar FA value $\leq 0.197 \times 10^{-3}$ mm^2/s, 95% CI = 0.679–0.930, the ROC curve showed an AUC of 0.831, with sensitivity of 77.8% and specificity of 81.8%. For prediction of renal normal clearance values (group A), using a threshold medullar FA value $>0.23 \times 10^{-3}$ mm^2/s, the ROC curve showed an AUC of 0.853, 95% CI = 0.706–0.945, with sensitivity of 80% and specificity of 80%.

4. Discussion

Several authors have investigated the role of DTI for evaluation of normal and injured kidneys. Gurses et al. and Wang et al. showed the feasibility of renal diffusion tensor imaging and repeatability of FA measurements [13,14]. Other authors tried to correlate DTI parameters measurements to renal function in patients with chronic kidney diseases [15–17]. In particular, all these authors agree that decrease of FA values of renal parenchyma reflects severity of renal damage. Liu et al. found a
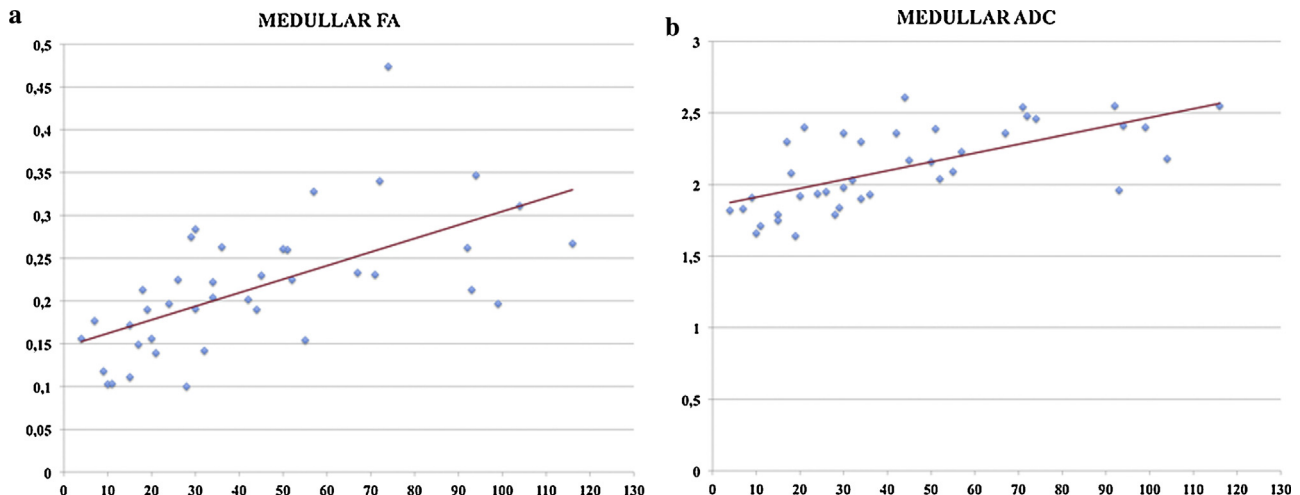

Fig. 6. Scatter diagrams of Pearson correlation between medullar FA and ClCr (a), and medullar ADC and CrCl (b), both showing a strong correlation (respectively $r = 0.62$ and $r = 0.66$).
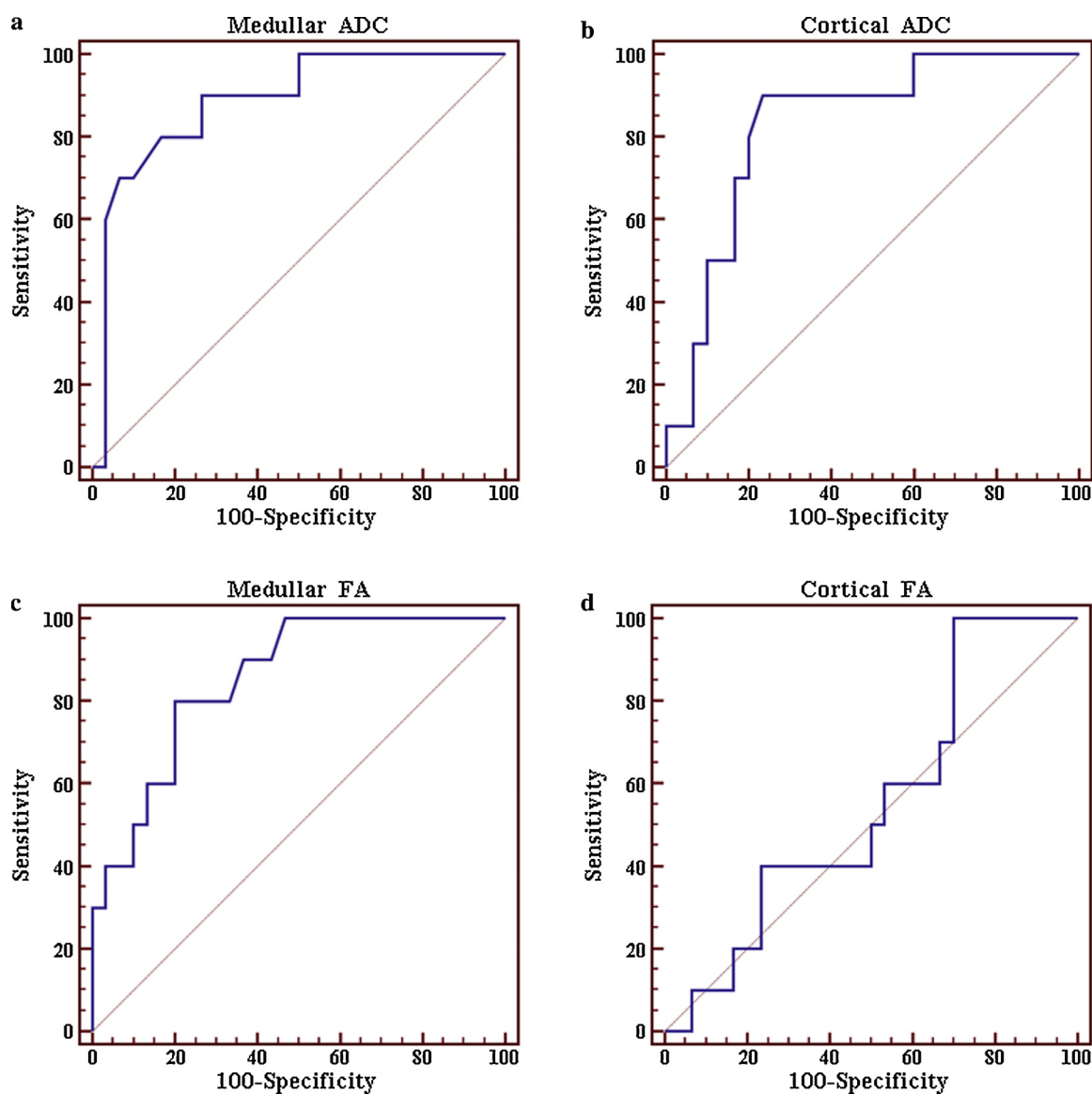
Fig. 7. ROC curves in prediction of group A: the ROC curve (a) shows an AUC of 0.871, with a sensitivity of 77.8% and specificity of 86.4% in the prediction of low creatinine clearance values (group C) using a threshold medullar ADC value $\leq 1.98 \times 10^{-3}$ mm^2/s. AUC of 0.814 (b), with a sensitivity of 72.2% and specificity of 86.4% was found using a threshold cortical ADC value $\leq 1.97 \times 10^{-3}$ mm^2/s. The ROC curve (c) shows an AUC of 0.831, with a sensitivity of 77.8% and specificity of 81.8% using a threshold medullar FA value $\leq 0.197 \times 10^{-3}$ mm^2/s. Finally (d) an AUC value of 0.527, with a sensitivity of 27.8% and specificity of 86.4%, was reported using a threshold cortical FA value $\leq 0.178 \times 10^{-3}$ mm^2/s.

positive correlation between FA and eGFR (estimated glomerular filtration rate): $r = 0.689$ for cortex and $r = 0.696$ for medulla [15]. Wang et al. demonstrated that cortical and medullar ADC and FA values were significantly lower in patients with chronic kidney disease than those of healthy volunteers: these values showed negative correlation with serum creatinine and blood urea nitrogen [16]. Gaudiano et al. investigated the role of FA values in a wide spectrum of chronic kidney diseases, showing that only medullary FA could be a marker of renal structural integrity alterations [17].

In addition, Lu et al. studied early changes of DT parameters in diabetic nephropathy finding lower mean medullary FA and ADC values among diabetics with relatively intact renal function (eGFR $\geq$ 60 ml/min/1.73 m^2) compared to healthy controls.

These findings suggest that medullary both FA and ADC may identify early changes in diabetics [18].

Diffusion MRI has been used also to evaluate renal allograft function [19–21]. Palmucci et al. evaluated the role of ADC measurements in transplanted kidney finding an ADC threshold $\geq 2.08 \times 10^{-3}$ mm^2/s to predict a normal clearance, although a certain overlap between groups [19].

Hueper et al. studied DTI as non-invasive tool for detection of allograft dysfunctions finding a significant reduction of medullar FA in transplanted kidneys compared to healthy volunteers. They also found a strong correlation between mean FA in the medulla and eGFR ($r = 0.72$) [20].

In a recent work by Lanzman et al. [21], the relationship between FA, ADC and renal function was analyzed.
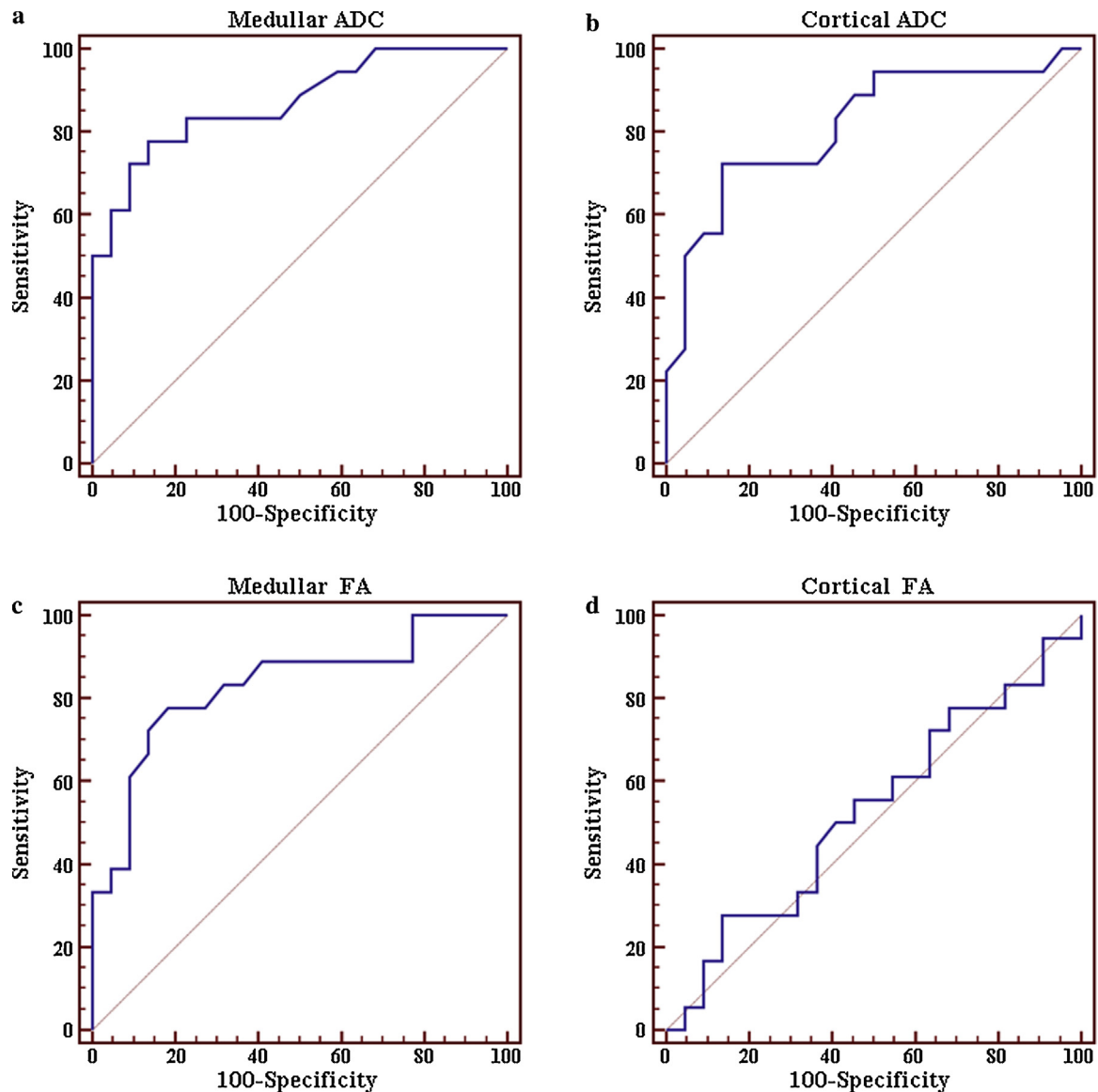
Fig. 8. ROC curves in prediction of group C: the ROC curve (a) shows an AUC of 0.885, with a sensitivity of 80% and specificity of 83.3% in the prediction of normal creatinine clearance values (group A) using a threshold medullar ADC value >2.3 × 10^{-3} mm^2/s. AUC of 0.832 (b), with a sensitivity of 90% and specificity of 76.7% was found using a threshold cortical ADC value >2.16 × 10^{-3} mm^2/s. The ROC curve (c) shows an AUC of 0.853, with a sensitivity of 80% and specificity of 80% using a threshold medullar FA value >0.23 × 10^{-3} mm^2/s. Finally (d), an AUC value of 0.550, with a sensitivity of 100% and specificity of 30%, was reported using a threshold cortical FA value >0.179 × 10^{-3} mm^2/s.

They divided patients into two groups according to eGFR: group A (eGFR > 30 mL/min/1.73 m^2) and group B (eGFR ≤ 30 mL/min/1.73 m^2). Cortex and medulla ADC values showed higher values in patients of group A, compared with patients with impaired function [21]. Mean FA values for cortex and medulla were significantly higher in group A (0.39 ± 0.06 and 0.17 ± 0.4), in comparison with group B (0.27 ± 0.05 and 0.14 ± 0.03) [21]. There was significant correlation between eGFR and medullary FA, with a *r* value of 0.65 ($p < 0.01$) [21].

Several theories have been proposed to explain water diffusion reduction in renal diseases.

In cases of renal dysfunction, filtration rate is low and water transport processes decrease [22]. All pathogenetic features of graft rejection, such as inflammation, edema, necrosis and

fibrosis [23], decrease renal water content, perfusion and interstitial spaces reducing molecular extracellular free diffusion and resulting in a decrease of ADC [7].

Namely, in interstitial fibrosis, collagen deposition narrows spaces between tubuli, and water diffusion becomes reduced. Recent experience by Togao et al. has already confirmed this fact: these researchers stopped ureteral excretion in rats to evaluate ADC behavior in renal fibrosis. They found an ADC decrease related to an increased number of cells, including fibroblasts, concluding that "ADC has the potential to serve as a sensitive noninvasive biomarker of renal fibrosis" [24]. Also Zhao et al., in a recent study, correlated pathological fibrosis score with ADC decrease in patients with chronic renal diseases, finding a good correlation [25].

In our study, the Mann–Whitney *U* test revealed a highly significant difference ($p < 0.01$) between patients with low CrCl (group C) and normal CrCl (group A) considering both medullar ADC and FA and cortical ADC. Regarding contiguous groups, difference between patients with intermediate creatinine clearance (group B) and patients of group C was highly significant ($p < 0.01$) for medullar ADC and significant ($p < 0.05$) for cortical ADC and medullar FA. No difference between these groups was found considering cortical FA. Analyzing groups A and B, we found a significant difference ($p < 0.05$) for medullar both ADC and FA, while no difference was found for cortical ADC and FA.

We found a good correlation between creatinine clearance and medullar ADC ($r = 0.65$), and between creatinine clearance and medullar FA ($r = 0.62$). A moderate correlation was observed between creatinine clearance and cortical ADC ($r = 0.56$), while cortical FA did show no correlation. In contrast with previous study of Lanzman et al. [21], cortical FA values were not significantly different in our Mann–Whitney analysis; a certain degree of overlap was observed, with medians of 0.211 in group A, 0.226 in group B and 0.208 in group C. Probably, different repartition of patients could explain this degree of overlap; however, it has to be noted that cortical FA did not show correlation also in the previously mentioned study by Lanzman [21].

In both prediction of group C and group A, medullar ADC revealed the best accuracy, showing an AUC of 0.871, with sensitivity of 77.8% and specificity of 86.4%, but also medullar FA showed a high accuracy.

Limitations of this study were the small number of patients enrolled, as well as the absence of histopathologic correlation. In addition, a higher magnetic field strength would have provided a better signal-to-noise ratio, higher values of FA and better images quality [26–28].

A certain degree of overlap for ADC and FA values among the three different classes studied represents a limit.

Another limitation is that we used only six encoding directions: as demonstrated in a study by Chuck et al., a higher number of encoding directions results in better image quality and improved cortico-medullary discrimination, although it does not influence FA values. Although the longer acquisition time, "the increase in image quality allows for a more precise data evaluation when placing ROIs for FA measurements" [29].

5. Conclusion

These results emphasized the role of DWI in evaluation of transplanted kidney: medullar ADC resulted the best parameter for renal assessment, distinguishing between patients with good, moderate or impaired renal function. A medullar ADC value of 2.3 may be used as a threshold for predicting a normal clearance level. In our study, also medullar FA values good correlated with renal functionality, although in a slightly lower degree. However, a certain degree of overlap between ADC and FA values, among the three different classes, seems to limit use of functional MR in daily clinical practice.

References

[1] Franke M, Kramarczyk A, Taylan C, Maintz D, Hoppe B, Koerber F. Ecoguidata biopsia renale percutanea in 295 bambini e adolescenti: il ruolo della ecografia e analisi delle complicanze. PLOS ONE 2014;9(dicembre (12)):e114737.

[2] Perez-Rodriguez J, Lai S, Ehst BD, Fine DM, Bluemke DA. Nephrogenic systemic fibrosis: incidence, associations and effect of risk factor assessment – report of 33 cases. Radiology 2009;250(February (2)):371–7.

[3] Canga A, Kislikova M, Martìnez-Galvez M, Arias M, Fraga-Rivas P, Poyatos C, et al. Renal function, nephrogenic systemic fibrosis and other adverse reactions associated with gadolinium-based contrast media. Nefrologia 2014;34(4):428–38.

[4] Gilet AG, Kang SK, Kim D, Chandarana H. Advanced renal mass imaging: diffusion and perfusion MRI. Curr Urol Rep 2012;13:93–8.

[5] Paudyal B, Paudyal P, Tsushima Y, Oriuchi N, Amanuma M, Miiyazaki M, et al. The role of the ADC value in the characterisation of renal carcinoma by diffusion-weighted MRI. Br J Radiol 2010;83(April (988)):336–43.

[6] Faletti R, Cassinis MC, Fonio P, Grasso A, Battisti G, Bergamasco L, et al. Diffusion-weighted imaging and apparent diffusion coefficient values versus contrast-enhanced MR imaging in the identification and characterisation of acute pyelonephritis. Eur Radiol 2013;23(12):3501–8.

[7] Palmucci S, Mauro LA, Veroux P, Failla G, Milone P, Ettorre GC, et al. Magnetic resonance with diffusion-weighted imaging in the evaluation of transplanted kidneys: preliminary findings. Transplant Proc 2011;43(May (4)):960–6.

[8] Abou-El-Ghar ME, El-Diasty TA, El-Assmy AM, Refaie HF, Refaie AF, Ghoneim MA. Role of diffusion-weighted MRI in diagnosis of acute renal allograft dysfunction: a prospective preliminary study. Br J Radiol 2012;85(June (1014)):e206–11.

[9] Van AT, Granziera C, Bammer R. An introduction to model-independent diffusion magnetic resonance imaging. Top Magn Reson Imaging 2010;21(December (6)):339–54.

[10] Le Bihan D, Mangin JF, Poupon C, Clark CA, Pappata S, Molko N, et al. Diffusion tensor imaging: concepts and applications. J Magn Reson Imaging 2001;13(April (4)):534–46.

[11] Pagani E, Bammer R, Horsfield MA, Rovaris M, Gass A, Ciccarelli O, et al. Diffusion MR imaging in multiple sclerosis: technical aspects and challenges. AJNR Am J Neuroradiol 2007;28(March (3)):411–20.

[12] Fukuda Y, Ohashi I, Hanafusa K, Nakagawa T, Ohtani S, Annaka Y, et al. Anisotropic diffusion in kidney: Apparent Diffusion Coefficient measurements for clinical use. J Magn Reson Imaging 2000;11:156–60.

[13] Gürses B, Kiliçkesmez O, Tasdelen N, Firat Z, Gürmen N. Diffusion tensor imaging of the kidney at 3 Tesla MRI: normative values and repeatability of measurements in healthy volunteers. Diagn Interv Radiol 2011;17(December (4)):317–22.

[14] Wang WJ, Pui MH, Guo Y, Hu XS, Wang HJ, Yang D. MR diffusion tensor imaging of normal kidneys. J Magn Reson Imaging 2014;40(November (5)):1099–102.

[15] Liu Z, Xu Y, Zhang J, Zhen J, Wang R, Cai S, et al. Chronic kidney disease: pathological and functional assessment with diffusion tensor imaging at 3T MR. Eur Radiol 2015;25(March (3)):652–60.

[16] Wang WJ, Pui MH, Guo Y, Wang LQ, Wang HJ, Liu M. 3T magnetic resonance diffusion tensor imaging in chronic kidney disease. Abdom Imaging 2014;39(August (4)):770–5.

[17] Gaudiano C, Clementi V, Busato F, Corcioni B, Orrei MG, Ferramosca E, et al. Diffusion tensor imaging and tractography of the kidneys: assessment of chronic parenchymal diseases. Eur Radiol 2013;23(June (6)):1678–85.

[18] Lu L, Sedor JR, Gulani V, Schelling JR, O'Brien A, Flask CA, et al. Use of diffusion tensor MRI to identify early changes in diabetic nephropathy. Am J Nephrol 2011;34(5):476–82.

[19] Palmucci S, Mauro LA, Failla G, Foti PV, Milone P, Sinagra N, et al. Magnetic resonance with diffusion-weighted imaging in the evaluation of transplanted kidneys: updating results in 35 patients. Transplant Proc 2012;44(September (7)):1884–8.

[20] Hueper K, Gutberlet M, Rodt T, Gwinner W, Lehner F, Wacker F, et al. Diffusion tensor imaging and tractography for assessment of renal allograft dysfunction-initial results. Eur Radiol 2011;21(November (11)):2427–33.

[21] Lanzman RS, Ljimani A, Pentang G, Zgoura P, Zenginli H, Kröpil P, et al. Kidney transplant: functional assessment with diffusion-tensor MR imaging at 3T. Radiology 2013;266(January (1)):218–25.

[22] Ries M, Jones RA, Basseau F, Moonen CT, Grenier N. Diffusion tensor MRI of the human kidney. J Magn Reson Imaging 2001;14(July (1)):42–9.

[23] Park WD, Griffin MD, Cornell LD, Cosio FG, Stegall MD. Fibrosis with inflammation at one year later predicts transplant functional decline. J Am Soc Nephrol 2010;21(November (11)):1987–97.

[24] Togao O, Doi S, Kuro-o M, Masaki T, Yorioka N, Takahashi M. Assessment of renal fibrosis with diffusion-weighted MR imaging: study with murine model of unilateral ureteral obstruction. Radiology 2010;255(June (3)):772–80.

[25] Zhao J, Wang ZJ, Liu M, Zhu J, Zhang X, Zhang T, et al. Assessment of renal fibrosis in chronic kidney disease using diffusion-weighted MRI. Clin Radiol 2014;69(November (11)):1117–22.

[26] Seo Y, Wang ZJ, Morriss MC, Rollins NK, Minimum. SNR and acquisition for bias-free estimation of fractional anisotropy in diffusion tensor imaging – a comparison of two analytical techniques and field strengths. Magn Reson Imaging 2012;30(October (8)):1123–33.

[27] Lee SK. Diffusion tensor and perfusion imaging of brain tumors in high-field MR imaging. Neuroimaging Clin N Am 2012;22(May (2)):123–34, ix.

[28] Chung AW, Thomas DL, Ordidge RJ, Clark CA. Diffusion tensor parameters and principal eigenvector coherence: relation to b-value intervals and field strength. Magn Reson Imaging 2013;31(June (5)): 742–7.

[29] Chuck NC, Steidle G, Blume I, Fischer MA, Nanz D, Boss A. Diffusion tensor imaging of the kidneys: influence of b-value and number of encoding directions on image quality and diffusion tensor parameters. J Clin Imaging Sci 2013;3(November):53.